

## Effect of ambient aging during soybean meal storage on the performance of a soybean-based adhesive

Jin Li<sup>a,1</sup>, Ziwen Chang<sup>a,1</sup>, Binghan Zhang<sup>a</sup>, Xu Li<sup>a</sup>, Zongxing Sun<sup>a</sup>, Huo Pengfei<sup>a,\*</sup>, Shifeng Zhang<sup>b</sup>, Zhenhua Gao<sup>a</sup>

<sup>a</sup> Key Laboratory of Bio-Based Material Science and Technology (Ministry of Education), Northeast Forestry University, Harbin, 150040, China

<sup>b</sup> MOE Key Laboratory of Wooden Material Science and Application, Beijing Forestry University, Beijing, 100083, China

### ARTICLE INFO

#### Keywords:

Soybean meal  
Ambient aging  
Wood adhesive  
Structure-property relationship  
Bond property

### ABSTRACT

Ambient aging is a common phenomenon that occurs under ambient conditions during the storage and use of polymeric substances, which may significantly affect the product performance. The aging of soybean meal (SM) during storage and its effects on the structures and properties of both SM and SM-based adhesive were investigated. It is confirmed that the SM powder underwent significant aging in the 4 months after grinding, resulted from the oxidation, decomposition, repolymerization and rearrangement of the SM chains. The carbonyl concentrations on the surface and in the bulk of SM after aged for 6 months increased 31.6% and 20.5, respectively. The physicochemical changes of ambient-aged SM powder affected the SM-based adhesive by increasing wettability but lowering crosslink density. Three-layer plywood, bonded with ambient-aged SM adhesives, exhibited decreased shear strength and water resistance, mainly resulting from the decreased crosslink density of the cured adhesive upon the aging time of the SM powder. The 6-month ambient aging of SM caused dry strength reduced by 52.6% and aged wet strength decreased by 53.8%. As a result, ambient aging and its negative effects should be carefully taken into account by manufacturers and customers to avoid the ineffectiveness and instability of SM and SM-based adhesive.

### 1. Introduction

Urea-formaldehyde is one of formaldehyde-based synthetic adhesives, which is widely used in the wood industry because of its low cost, good bonding strength and acceptable water resistance (Liu et al., 2018). However, this synthetic adhesive is derived from nonrenewable fossil resources and release toxic formaldehyde (Sitz et al., 2017). Research on bio-based adhesives, from such biomasses as soybean protein, starch, and lignin, has attracted increasing attention in response to the crisis of resource depletion and environmental pollution.

Soybean protein is a desirable substitute for fossil resources in the preparation of nontoxic bio-adhesives in the wood industry, because it is naturally derived, abundant, low in cost, and renewable (Vnucecc et al., 2017; Kumar et al., 2002). However, traditional soybean protein-based adhesives exhibit insufficient bond strength and poor water resistance, due to their complicated quaternary structure and weak intermolecular interactions (Fahmy et al., 2010; Kumar et al., 2002). Many modification reagents, including denaturation reagents, reactive crosslinkers, and synthetic resins, are applied to improve the bond

properties of soybean-based adhesives, such as alkali (Wan and Chen, 2014), urea (Gao et al., 2012), sodium dodecyl sulfate (Huang and Sun, 2000), glycidyl methacrylate (Qin et al., 2013), maleic anhydride (Liu and Li, 2007), epichlorohydrin-modified polyamidoamine (EMPA) (Gu and Li, 2011), epoxy resin (Lei et al., 2014), phenol-formaldehyde resin (Tabarsa et al., 2011), melamine-urea-formaldehyde resin (Park et al., 2009) and polycaprolactone (Tous et al., 2019). Some bio-based derivatives reactive to soybean protein such as tannin (Ghahri and Pizzi, 2018; Ghahri et al., 2018a, 2018b) and soybean oil are also used (Sitz et al., 2017; Zhao et al., 2018). After modification, the physic-chemical properties of soybean meal and soybean-based adhesives generally changed, resulting in importantly improvements of bond strength and water resistance (Zhao et al., 2015; Zhong and Sun, 2000; Zhong et al., 2007). Nowadays, the modified soybean-based adhesives are able to withstand water soaking at 63 °C (2013; Lei et al., 2014; Qin et al., 2013; Zhao et al., 2018) and water boiling or even boiling-dry-boiling cycled treatments (Fan et al., 2016; Gao et al., 2015). Since 2005 Columbia Forest Products, USA, has been manufacturing formaldehyde-free hardwood plywood using a soybean-based adhesive derived from

\* Corresponding authors.

E-mail addresses: [huopengfei@nefu.edu.cn](mailto:huopengfei@nefu.edu.cn) (H. Pengfei), [gao\\_zhenhua@yahoo.com](mailto:gao_zhenhua@yahoo.com) (Z. Gao).

<sup>1</sup> These two authors contributed equally to this work and should be considered co-first authors.

food-grade soybean flour and a wet strength resin. In 2017, the issue of the more server Chinese Standard GB18580-2017 about formaldehyde release from wood composites promotes the increasing been application of soybean-based adhesives in the wood industry in China for composites manufacturing (e.g., plywood, blockboard, particleboard, and fiberboard), due to the additional advantages of environmental safety and improved technological applicability (Fan et al., 2016; Li et al., 2019).

Commonly, commercial soybean-based adhesive is a two-component formulation composed of SM powder and EMPA solution (as either crosslinker or disperser) (Frihart and Satori, 2013). These two components are stored independently and mechanically blended at room temperature to formulate the adhesive just before use. However, compared to adhesive from fresh EMPA solution and freshly ground SM powder, the bond strength and water resistance of the plywood prepared from fresh EMPA solution and stored SM powder (especially that stored for more than 3 months) deteriorated significantly. This occurrence is probably attributed to the ambient aging of SM powder during its storage. It is industrially important to understand what happens to SM powder during storage to avoid the ineffectiveness and instability of SM powder and SM-based adhesive.

Similar findings for the time-dependent physical and chemical changes of biopolymers, such as protein and/or wood, under ambient conditions have been reported (Bai and Gao, 2011; Ciannamea et al., 2015; Haque et al., 2015; Mo and Sun, 2003). The solubility of milk protein concentrate powder decreased while being stored at 25 °C for 14 weeks, due to the protein denaturation and intermolecular interaction of peptide chains during storage (Haque et al., 2015). It was reported that the mechanical properties of medium-density fiberboard were greatly decreased when made with ambient-aged wood fibers. This is attributed to the poor wettability between adhesives and the surface-varied fibers (Bai and Gao, 2011). The storage-induced functional property changes of soybean protein concentrate films was studied; the reorganization of protein secondary structures and the molecular interactions via disulfide crosslinks and/or Maillard aggregates were observed during 90-day storage (Ciannamea et al., 2015). Additionally, reports indicated that soybean protein isolate plastics had gradually decreased tensile strengths over the course of storage for 180 days at 25 °C, due to the enthalpy of relaxation (Mo and Sun, 2003). These works confirmed that many types of biomass suffers ambient aging during storage, which may significantly affect the service life and quality stability of commercial biomass-based products, due to deteriorated performances.

However, to our knowledge, no study has yet been reported on the ambient aging of SM powder and its effects on the properties of SM-based adhesives. In the current study, freshly ground SM powder was subjected to ambient aging for 6 months under the following conditions: ambient temperature (20–30 °C), relative humidity (40–60%), no direct sunshine, and ventilation. The physicochemical properties of SM powder and SM-based adhesive with various aging times were systematically evaluated by means of Fourier transform infrared analysis (FTIR, both transmission and reflection modes), X-ray photoelectron spectroscopic (XPS) analysis, gel permeation chromatographic (GPC) analysis, thermogravimetric analysis (TGA), X-ray diffraction (XRD) analysis, sol-gel testing, contact angle measurements, functional group determination, and mechanical testing of the SM-based adhesive-bonded plywood, which inform the mechanisms of the SM powders' ambient aging and its effects on the SM-based adhesives for industrial applications.

## 2. Materials and methods

### 2.1. Materials

Soybean meal (SM) with 43.5% soy protein content was obtained from Laihe Oil Pressing Factory (Shandong, China). The SM was

ground to a fine powder that passed through a 160-mesh sieve using a high-speed crusher. EMPA solution as crosslinker was synthesized from diethylenetriamine, adipic acid, and epichlorohydrin in our lab, and had a solid content of 13.4%, a pH value of 3.2, and a viscosity of 68 MPa s (25 °C). Urea and other chemicals at reagent grade were obtained from Tianjin Komio Chemical Co. Ltd. (Tianjin, China). Birch veneers with dimensional size of 420 mm × 420 mm, thickness of 1.6 mm and moisture content of 6–8% were provided by Weihe Fulin Plywood Plant (Heilongjiang, China).

### 2.2. Ambient aging and thermal oxidative aging of SMs

The freshly ground SM powders were placed into an open enamel container with a sample thickness of approximately 1 mm, and then subjected to ambient aging under the following conditions: ambient temperature (20–30 °C), relative humidity (50–70%), no sunshine, and ventilation. The SM powder was sampled and ground monthly for six consecutive months. Six ambient-aged samples, with aging times of 1, 2, 3, 4, 5, and 6 months (labeled as SM-1 m, SM-2 m, SM-3 m, SM-4 m, SM-5 m and SM-6 m), were obtained. A freshly ground SM sample was taken as the control for characterization.

### 2.3. Preparation of SM-based adhesives

Prior to adding 35 g of SM powder (35 g), 89.55 g of EMPA solution in beaker was blended with 10.45 g of deionized water to adjust its solid content to 12.0 wt%. The above mixture was mechanically stirred at room temperature and rotating speed of 200 rpm for 5 min to form a nongranular SM-based adhesive with a solid content of 32.5 wt%. SM-6 m, SM-5 m, SM-4 m, SM-3 m, SM-2 m, SM-1 m and fresh SM were used to prepare the corresponding adhesive samples.

### 2.4. Fourier transform infrared (FTIR) analysis of SMs with transmission and reflection modes

All SM samples were FTIR analyzed with transmission and reflection modes to evaluate the chemical structures of SM samples on their surfaces and in bulk. Transmission-FTIR was performed after mixing the SM sample with potassium bromide crystals at a mass ratio of approximately 1/150 and molding into a transparent FTIR disk. A reflecting accessory was equipped to obtain reflection-FTIR spectra that detected the chemical structures of each sample at approximately 5 nm thickness. The two modes of FTIR spectra were recorded using a Nicolet 7600 spectrometer (Nicolet Instrument Corp., Madison, WI) from 500 to 4000  $\text{cm}^{-1}$  with a 4  $\text{cm}^{-1}$  resolution and 32 scans. The relative IR absorbance of the carbonyl group of SM with various aging times was determined according to the Lambert-Beer law by taking the C–H peak at approximately 2912  $\text{cm}^{-1}$  as an internal standard (Gao et al., 2015).

### 2.5. X-ray photoelectron spectroscopic (XPS) analysis of SMs

Each SM sample was powdered and analyzed by an ESCALAB250 XPS apparatus (Thermo Fisher Scientific) equipped with an Al-K source. All XPS spectra were recorded with 0.1 eV step and 20 eV pass energy. Curve-fitting analyses of the C 1s, N 1s and O 1s peaks were performed with Casa XPS 2.3.16 software.

### 2.6. Gel permeation chromatographic (GPC) analysis of SMs

A reaction kettle equipped with mechanical stirrer and refluxing equipment was charged with 5 g of SM and 100 g of urea solution (8 mol/L). The mixture was maintained at  $50 \pm 2$  °C for 2.5 h with stirring to dissolve the SM protein completely, during which partial urea might convert to ammonia by the urease in the SM without deenzyming or thermal treatment; however the urea concentration (8 mol/L) was sufficient for complete dissolution of SM sample. After

that, the resultant product was cooled to room temperature and then filtered with a glass fiber filter. The filtered solution was then diluted to 0.1 wt% with deionized distilled water before the determination of the molecular weight (MW) using an Agilent 1100 GPC equipped with a differential refraction detector and two chromatographic columns in series (namely, 79911GF-083, with a MW ranging from 100 to 30k, and 79911GF-084, with a MW range from 10k to 200k). The mobile phase was 4.8 wt% (0.8 mol/L) urea solution with a flow rate of 1 mL/min, and the pressure on the columns was 78 psi. The GPC was calibrated with 4 standard polysaccharides produced by Polymer Laboratories, USA. These polysaccharides have MWs of 12000, 50000, 150000, and 410000, and their distribution indexes ranged from 1.0 to 1.05.

### 2.7. X-ray diffraction (XRD) analysis of SMs

All SM powder was evaluated in a D/max-2200 diffractometer (Rigaku International Corporation, Tokyo, Japan) using a Cu-K $\alpha$  source. The data were collected from 5 to 50° with a step interval of 0.02°, an accelerating voltage of 40 kV and a current of 30 mA.

### 2.8. Acetaldehyde value test of SMs

The acetaldehyde value represents the content of reactive amino groups of the SM, which was defined as the equivalent moles of acetaldehyde (mmol) that can react with 1 g of solid SM, and was determined as reported (Li et al., 2019).

### 2.9. Apparent viscosity and water content of SM-based adhesives

The apparent viscosity of the adhesive was tested with a Brookfield DV-II Pro viscometer (USA) at 25 °C with an S64 spindle at a rotating speed of 3.0 rpm. The average value of three tests was recorded.

To determine the water content of the liquid SM-based adhesives, each sample was placed between two glass fiber filters attached to cotton filter papers to absorb free water from the adhesives. Samples were squeezed by hand to remove most free water by replacing the cotton filter papers until no more moisture appeared. The squeezed sample ( $m_2$ ) was immediately placed in an oven at  $103 \pm 2$  °C to dry until reaching consistent weight ( $m_3$ ). The water content was calculated by  $(m_2 - m_3)/m_3 \times 100\%$ .

### 2.10. Contact angle of SM-based adhesives

The contact angle was measured using a Theta optical contact angle meter (Biolin Scientific, Sweden). Thirty seconds after a liquid adhesive drop was placed onto a birch veneer surface at room temperature (23–25 °C) and a relative humidity of 50–60%, the shape of the sample was recorded by a CCD video camera. The contact angle was determined by fitting the Young-Laplace equation to the drop profile. The data presented in this study is an average of seven replicated tests.

### 2.11. Sol-gel test and thermogravimetric analysis (TGA) of cured SM-based adhesives

The cured SM-based adhesive (at  $120 \pm 2$  °C for 6 h) was then ground into fine powder passed through a 160-mesh sieve. Approximately 2.0 g of cured adhesive powder ( $m_4$ , accurate to 0.0001 g) and 200.0 g of distilled water were added into a 250-mL flask, and the mixture was kept stirring and boiling for 4 h under refluxing. The dispersion was then cooled to room temperature and filtered. The residue on the glass-filter paper ( $m_5$ , accurate to 0.0001 g) was rinsed twice with 50 ml of distilled water before oven-dried at 120 °C to a constant weight ( $m_6$ , accurate to 0.0001 g). The crosslinking density in terms of gel content was defined as the mass percentage of SM that was insoluble in boiling water and was calculated by  $[(m_6 - m_5)/m_4] \times 100\%$ ; the sol content was calculated by  $[1 - (m_6 - m_5)/m_4] \times 100\%$ .

Each finely powdered, cured SM-based adhesive was subjected to TGA analysis using a Netzsch 209 F3 TGA instrument from room temperature to 600 °C at a heating rate of 10 °C /min under a nitrogen purge of 25 mL/min.

### 2.12. Evaluation of bond properties of SM-based adhesives

Three-ply plywood panels for evaluating bond properties were manufactured with an adhesive dosage of 180 g/m<sup>2</sup> for each glue line, by coating the adhesive onto both surfaces of the core veneer. In order to avoid variability of wood, the veneers used were selected with grains and texture as similar as possible. All plywood panels were veneers used. The adhesive-coated veneer was stacked between two uncoated veneers with their grain directions perpendicular to each other before hot-pressed at 120 °C and 1.3 MPa for 4 min. Two plywood replicates were prepared with each adhesive. The plywood panels kept under ambient conditions for at least 24 h prior to property evaluation.

A total of 60 specimens were cut and sampled from two replicated panels with a bond area of 25 mm  $\times$  25 mm in accordance with ASTM D906-2017. The bond properties of plywood for interior use (Type II plywood, soaked bond strength) and for structural use (Type I plywood, aged bond strength) were determined according to the Chinese standard GB/T 17657-2013 with a strain rate of 5 mm/min at a gauge length of 50 mm. For aged bond strength test, 20 specimens was subjected to a hygrothermal treatment (4 h of boiling, 20 h of oven-drying at  $63 \pm 2$  °C, and another 4 h of boiling) before shear-strength test in the wet state; and another 20 specimens were soaked in water at  $63 \pm 2$  °C for 3 h before shear-strength test in the wet state for determination of soaked bond strength according to the Chinese standard GB/T 17657-2013.

### 2.13. Statistical analysis

The data in the current study are reported as the mean value  $\pm$  standard deviation. Single factor analysis of variance was conducted to differentiate significant differences among mean values of the data, and p-values < 0.05 were regarded as statistically significant.

## 3. Results and discussion

### 3.1. Effects of ambient-aging time on physicochemical structures of SMs

The aging of a substance may result in structural changes. The FTIR analysis in Fig. 1A shows that the aged and fresh SMs had quite similar IR absorption peaks with some intensity variations. The N–H/OH–stretching of amino and hydroxyl groups was detected at 3430 cm<sup>-1</sup> in transmission mode but shifted to 3280 cm<sup>-1</sup> in reflection mode, attributed to the blueshift phenomenon resulting from varied intermolecular interactions, such as hydrogen bonding, at the sample surface and in the bulk. The main absorptions, at approximately 1650, 1537, and 1243 cm<sup>-1</sup>, were associated with the characteristic amide I (C=O stretching), amide II (NH– bending) and amide III (C–N stretching/NH– bending) of proteins, respectively (Liu et al., 2017). The band at 1050 cm<sup>-1</sup> was related to CN–H<sub>2</sub> bending (Luo et al., 2017).

It is well known that FTIR analysis in transmission mode detects the average group concentration through the sample thickness, while its reflection mode detects those within roughly ten atoms of the sample surface (Al-Qadiri, 2011). Because protein aging is associated with changes of the carbonyl groups (Hipkiss et al., 2001), quantitative results in Fig. 1B indicated that both the carbonyl concentrations (or relative IR absorbance) on the surface and in the bulk of SMs increased with ambient aging time, and the carbonyl concentration on the sample surface was higher than that in the bulk. In addition, the carbonyl quantity on the surface increased quickly in the first 3 months but much slowly later, while that in the bulk increased gradually but consistently over 6 months. These facts indicated that the ambient aging was time-

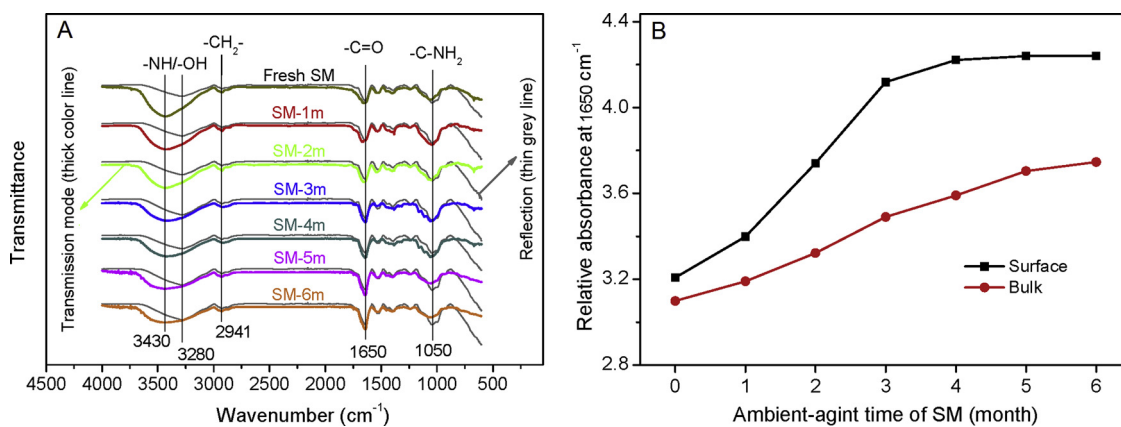


Fig. 1. FTIR analysis of SM samples with various ambient-aging times.

Table 1

Elemental compositions of SM with various ambient-aging times by XPS.

Sample	C (area %)	N (area %)	O (area %)	C/O *
Fresh SM	75.3	5.5	19.2	3.9
SM-1m	74.2	5.9	19.9	3.7
SM-2m	73.9	6.0	20.1	3.7
SM-3m	73.2	6.0	20.8	3.5
SM-4m	73.2	5.8	21.0	3.5
SM-5m	72.9	5.4	21.7	3.4
SM-6m	71.4	5.6	23.1	3.1

Note: C/O ratio refers to the mole ratio calculated as (peak area of C/sensitivity factor 0.296) / (peak area of O/sensitivity factor 0.711).

dependent, starting on the sample surface after grinding SM and then gradually moving deep into the interior bulk after some time.

XPS analysis, detailed in Table 1, showed that the areas of  $C_{1s}$  peaks decreased; those of  $O_{1s}$  increased upon aging time, resulting in an ever-decreasing C/O ratio, further confirming the formation of carbonyl groups during ambient aging. The concentration of N slightly increased until 3 months and then decreased, indicating that N-containing groups in SM, such as amino and amide groups, were more stable compared with groups that were able to convert to carbonyl groups. According to similar findings on the aging process of some biomasses such as proteins (Catalgol et al., 2012; Reeg and Grune, 2015) and wood (Bai and Gao, 2011), the formation of carbonyl groups during the 6-month aging of SMs under ambient conditions was mainly due to the slow chain oxidation by oxygen of alcoholic hydroxyl and alkyl groups into carbonyl groups, as illustrated by Eqs. (1)–(4) in Fig. 2.

To investigate the detailed oxidation reactions, the peaks of  $C_{1s}$ ,  $N_{1s}$  and  $O_{1s}$  were further subdivided by curve fitting (Fig. 3) and then identified (Table 2) according to the reported bond energies of each fixed sub-peak (Guerrero et al., 2013, 2014; Li et al., 2015b; Zhang et al., 2017). The  $C_{1s}$  peak of SM could be divided into three sub-peaks, corresponding to C1 (C–C/CH, 284.6 eV), C2 (CO/CN, 286.0–286.1 eV), and C3 (CO, 287.5–287.9 eV). The changes of their sub-peak contents according to their peak areas shown in Table 2 indicated that the decrease of element C upon aging time was attributing to the conversion of alkyl groups (C–H/CC) into CO and CO groups. However, the formation of C=O groups were much more than that of CO groups because the sub-peak C3 had 46.1% increment, from 12.59 area% of fresh SM to 18.39 area% of SM-6 m, while the sub-peak C2 had only an 18.0% increment, from 25.22 area% of fresh SM to 29.77 area% of SM-6 m. This fact implied that the ambient aging of SM mainly resulted from chain oxidation, as illustrated by Eqs. (5)–(7) in Fig. 2.

The  $O_{1s}$  peak of SM could also be divided into three sub-peaks, corresponding to O1 (O–CO / OCN, 530.3–530.7 eV), O2 (COC / COH,

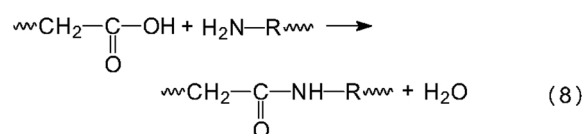
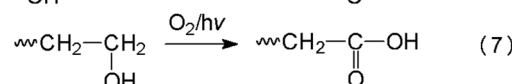
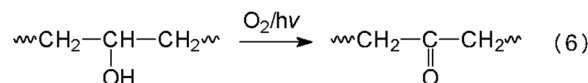
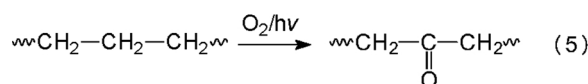
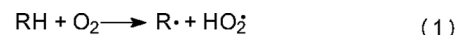


Fig. 2. Illustration of chain oxidation of SM during its ambient aging.

531.6–531.9 eV), and O3 ( $\text{H}_2\text{O}$ , 532.8–533.6 eV) (Guerrero et al., 2013, 2014; Li et al., 2015b; Zhang et al., 2017). The content changes of sub-peak O1 and O2 in Table 2 evidenced that some alcoholic hydroxyl groups of SM (represented by C–OH) were oxidized to form carbonyl and/or carboxyl groups as illustrated by Eqs. (6)–(7) in Fig. 2. SM contains approximately 40 wt% carbohydrates with abundant alcoholic hydroxyl groups for oxidation (Guerrero et al., 2013). The decreasing absorption intensity at  $3430\text{ cm}^{-1}$  in Fig. 1A upon aging time also confirmed the consumption of alcoholic hydroxyl groups during chain oxidations. The gradual increase of peak O3 was attributed to the water absorbed by SM from air (Guerrero et al., 2013), as evidenced by the corresponding moisture content of SM with various aging times, shown in Fig. 4B.

The subdivision and identification of  $N_{1s}$  peaks, corresponding to N1 (N–H, 398.5–399.1 eV), N2 (CN / NC, 399.2–399.6 eV), and N3 [NCO, 400.6–401.3 eV] (Guerrero et al., 2014; Zhang et al., 2017). The content of amino groups represented by sub-peak N1 was decreased while that of amide groups represented by N3 sub-peak increased upon the ambient-aging time, indicating that condensation between amino groups and carbonyl groups occurred as illustrated by Eq. (8) in Fig. 2.

GPC analysis in Fig. 4A shows that the fresh SM had a main GPC peak with peak MW of 434100 and a small satellite peak with peak MW of 268000, while the aged SM had two main peaks, with one larger

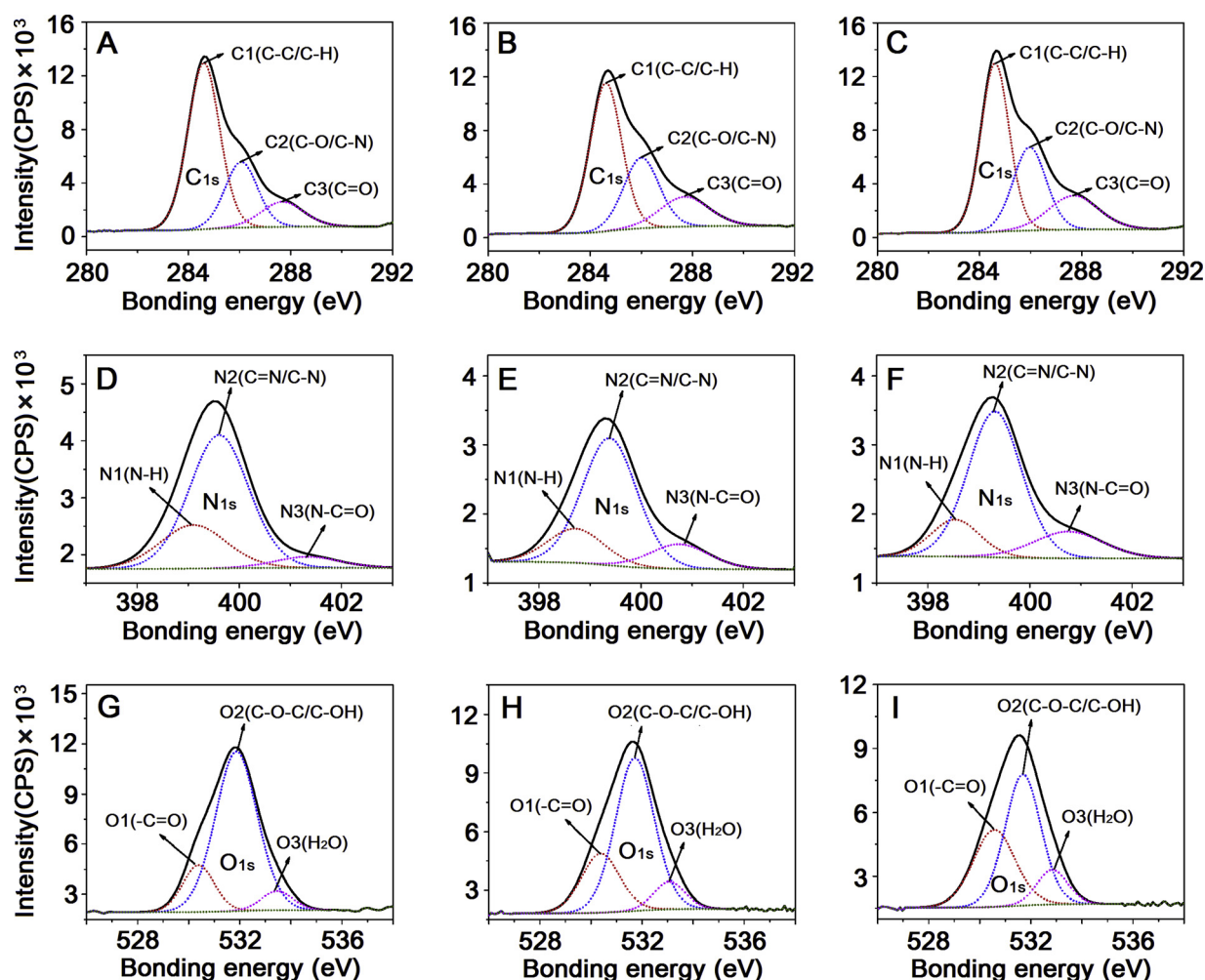


Fig. 3. Sub-peak fixings of  $C_{1s}$ ,  $N_{1s}$  and  $O_{1s}$  of SM samples by XPS (A, D and G refers to fresh SM; B, E and H relates to SM-3 m; C, F and I relates to SM-6 m).

peak MW of 590100 and one smaller MW of 333700. The number-averaged MW of SMs showed increasing tendency from 369100 to 385200 during 6 months of ambient aging. This implied that both decomposition and repolymerization took place simultaneously during ambient aging, but the repolymerization played a major role. It has been reported that protein oxidation leads to a partial unfolding and, therefore, releases some buried reactive groups in the globular structure of protein (Catalgol et al., 2012; Reeg and Grune, 2015). In addition, some new reactive groups, such as carbonyl groups, were generated from protein oxidation as illustrated by Eqs. (3) and (7) in Fig. 2. As a result, the repolymerization could be promoted by these reactive groups, further evidenced by the continuous consumption of amino

groups or the ever-decreasing acetaldehyde value of SMs from 0.061 mmol/g to 0.048 mmol based on ambient-aging time, as shown in Fig. 4B.

XRD analysis in Fig. 4C shows that the  $2\theta$  of SMs slightly decreased from  $20.3^\circ$  to  $19.9^\circ$ , while their crystallinities increased from 14.60% to 17.75%, upon ambient aging, indicating that the processes of repolymerization and the unfolding of the globular structure could result in regular rearrangements of SM chains or more compact structures during ambient aging. However, the percentage of regular rearrangements on the basis of total SM structures was relatively small, because aging mainly occurred on the surface of SM particles, as evidenced by both the small crystalline changes and reduced carbonyl formation in

Table 2

Peak areas, bond energy and assigned groups of each sub-peaks of  $C_{1s}$ ,  $N_{1s}$  and  $O_{1s}$ .

Sample	XPS peak	$C_{1s}$			$N_{1s}$			$O_{1s}$		
		C1	C2	C3	N1	N2	N3	O1	O2	O3
	Sub-peak	C1	C2	C3	N1	N2	N3	O1	O2	O3
	Assigned groups	C-C C-H	C-O C-N	C=O	N-H	C=N C-N	N-C=O	O=C=O O=C-N	C-O-C C-OH	H <sub>2</sub> O
	Bond energy (eV)	284.6	286.0	287.7	399.0	399.6	400.8	530.4	531.9	533.4
Fresh SM		62.19	25.22	12.59	25.08	68.75	6.17	16.97	76.15	6.88
SM-1m		58.25	27.05	14.70	24.38	65.49	10.12	20.86	71.69	7.45
SM-2m		56.00	28.21	15.79	16.33	71.17	12.50	21.64	69.93	8.43
SM-3m	Peak area (%)	54.15	28.97	16.87	18.66	67.21	14.14	25.05	65.40	9.55
SM-4m		52.76	29.29	17.95	14.84	69.91	15.26	29.03	60.93	10.04
SM-5m		51.98	29.72	18.30	16.73	67.08	16.19	35.05	53.25	11.69
SM-6m		51.83	29.77	18.39	15.77	68.03	16.22	35.97	52.14	11.88

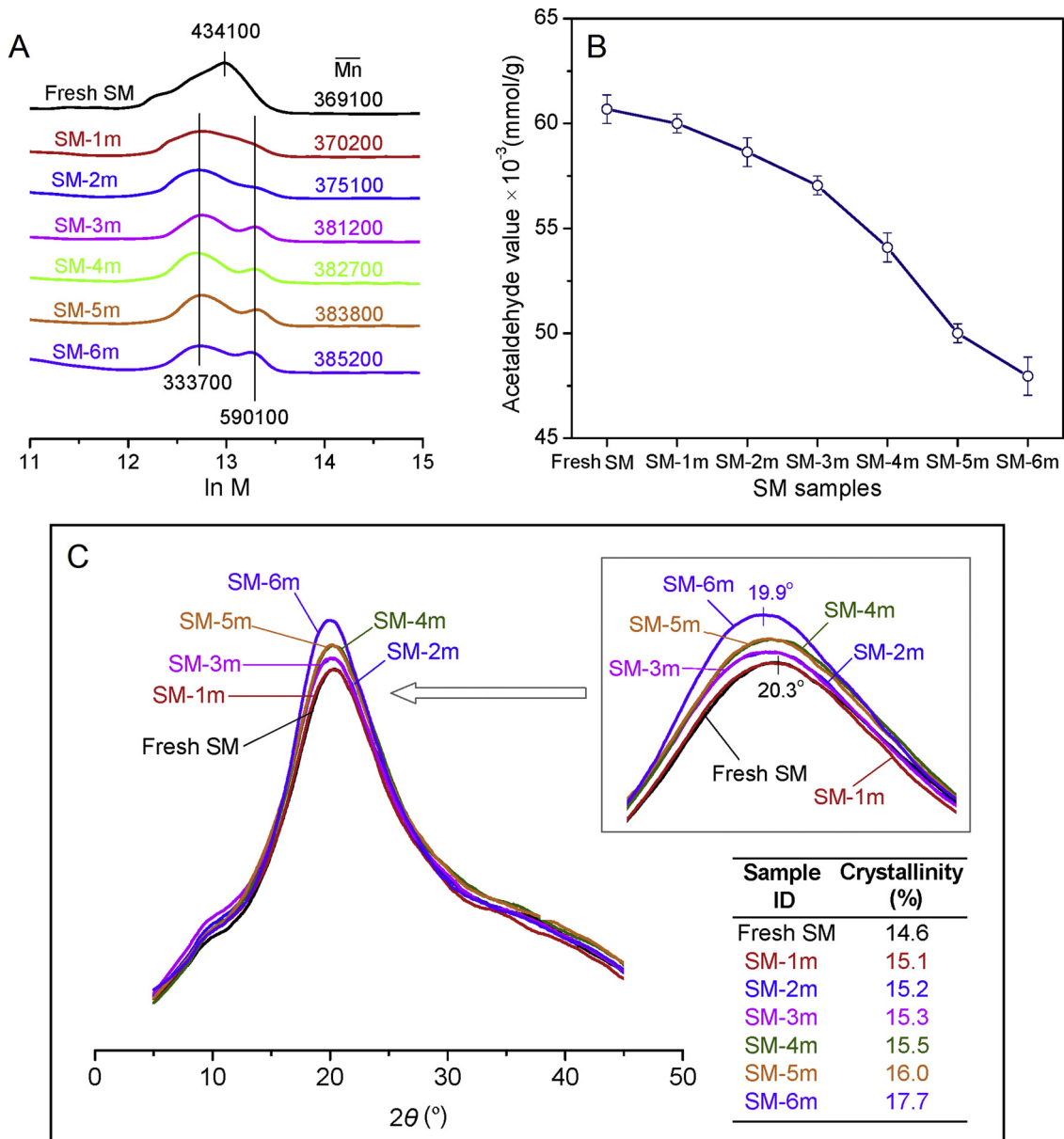


Fig. 4. GPC analysis, acetaldehyde value, moisture content and XRD analysis of SM with various ambient-aging times.

the SM bulk, as shown in Fig. 1B.

### 3.2. Effects of ambient aging on the physicochemical properties of SM-based adhesives

In general, the physicochemical properties of a substance are related to structural changes due to aging. The plywood evaluations of SM-based adhesives prepared with SM with various ambient-aging times are summarized in Table 3, indicating that the bond properties of these SM-based adhesives declined significantly as the ambient-aging time increased from 0 (freshly ground) to 6 months. Within the 6-month ambient aging, their dry strengths were reduced by 52.6% (from 3.46 to 1.64 MPa); soaked wet shear strength dropped by 39.0% (from 1.46 to 0.89 MPa) and aged bonding strength decreased by 53.8% (from 0.93 to 0.43 MPa). The SM-based adhesive prepared with freshly ground SM had the desired soaking bond strength for interior use (Type II plywood, > 1.0 MPa, according to Chinese standard GB/T 9846-2015) and a good aged bond strength for floor substrates (Type I plywood, > 0.7 MPa, according to Chinese standard LY/T 1738-2008).

**Table 3**  
Bond properties of SM-based adhesive with various ambient-aging times.

Sample ID	Dry strength (MPa)	Soaked bond strength (MPa)	Aged bond strength (MPa)	Number of delaminated specimens*
Fresh SM	3.46 ± 0.51 a	1.46 ± 0.08 a	0.93 ± 0.06 a	0, 0
SM-1m	3.10 ± 0.34 ab	1.33 ± 0.12 b	0.91 ± 0.20 a	0, 0
SM-2m	2.86 ± 0.30 b	1.32 ± 0.12 b	0.72 ± 0.15 b	0, 0
SM-3m	2.44 ± 0.42 c	1.12 ± 0.11 c	0.50 ± 0.17 c	0, 2
SM-4m	2.03 ± 0.25 d	1.13 ± 0.11 c	0.51 ± 0.23 c	0, 4
SM-5m	2.01 ± 0.21 d	1.13 ± 0.15 c	0.45 ± 0.11 d	12, 16
SM-6m	1.64 ± 0.26 e	0.89 ± 0.14 d	0.43 ± 0.03 d	16, 18

Note: Data in the table are means ± standard deviation of their replicates. The different letters (a, b, c, d, and e) indicate data that are significantly different at p-values < 0.05. Number of delaminated specimens refers to the number of specimens that delaminated in the first and second 4 h water-boiling, respectively, during the hygrothermal treatment of 20 specimens.

**Table 4**  
Main physicochemical properties of SM-based adhesive with various ambient aging times.

Sample	Droplet image	Contact angle (°)	Viscosity (mPa.s)	Water content (%)	Sol content (%)
Fresh SM		58.4 ± 0.9a	81010 ± 955a	64.0 ± 0.2a	23.6 ± 0.2a
SM-1 m		54.7 ± 1.0b	56517 ± 1188b	63.3 ± 0.4a	24.2 ± 0.1b
SM-2 m		51.2 ± 1.3c	49800 ± 1134c	62.2 ± 0.4b	24.5 ± 0.1c
SM-3 m		45.9 ± 0.9d	35877 ± 1086d	61.8 ± 0.2bc	25.2 ± 0.1d
SM-4 m		40.6 ± 1.2e	28800 ± 648e	61.0 ± 0.3 cd	25.4 ± 0.1d
SM-5 m		35.3 ± 0.9f	22890 ± 547f	60.5 ± 0.1de	26.9 ± 0.1e
SM-6 m		33.1 ± 1.1f	21120 ± 993f	60.0 ± 0.3e	27.2 ± 0.1f

Note: Data in the table are means ± standard deviation of their replicates. The different letters (a, b, c, d, e and f) after data are significantly different at p-values < 0.05.

However, the plywood bonded with SM-based adhesive had decreased soaking bond strengths lower than the required value for interior use after ambient aging the SM for 5 months and decreased aged bond strengths lower than the required value for floor substrates after 2 months of SM ambient aging. In addition, the increased bondline damage or more delamination of plywood specimens during the two-cycle water boiling of hygrothermal treatment indicated that the adhesives prepared with ambient-aged SM had significantly decreased water resistance. These test results confirmed that the inferior bond strength and water resistance of the corresponding SM-based adhesive must be attributed to the ambient aging of SM.

The contact angle test in Table 4 showed that the SM-based adhesives had significantly decreased contact angles from 58.4° (fresh SM) to 33.1° (SM-6 m) upon the ambient aging of SM, indicating the improved wettability of SM adhesive on a polar wood substrate. This was mainly due to the increased hydrophilicity of aged SMs, resulting from the chain oxidation that converted hydrophobic alkyl groups into hydrophilic alcoholic hydroxyl and carbonyl groups, as confirmed by FTIR and XPS analyses (Fig. 1B and Table 2). The decreased viscosity of SM-based adhesive over aging time (Table 4) was beneficial for adhesive wetting to the wood substrate, because a lower viscosity reflects less intermolecular interactions and more chain movement. According to modern bond mechanisms, the improved wettability and the decreased viscosity of adhesive are beneficial to both bonding and bond properties (Li et al., 2017). However, the bond properties of SM-based adhesives in Table 3 were opposed to their wettability and viscosity, indicating that the wettability and viscosity played a minor role for the adhesion of ambient-aged SM adhesives.

GPC results in Fig. 4A shows a slight increase of the MW of SM upon aging time, which might theoretically result in increased adhesive

viscosity, as a higher MW corresponds to more intermolecular interactions including hydrogen bonds and entanglements. The decreased viscosity of aged SM adhesives was attributed to weakened molecular interactions, since the SM chains rearranged during ambient aging and increased in crystalline area, as indicated by the higher crystallinity of the aged SM shown in Fig. 4C. This increased crystallinity trapped some free SM chains and restricted their intermolecular interactions. This could also be evidenced by the decreased water content of squeezed SM-based adhesive (Table 4), reflecting the content of water bound by free SM chains. The increased regular rearrangement also restricted the penetration of crosslinker EMPA within the “crystalline area” of SM. The crosslinking of SM adhesive by crosslinker EMPA was mainly due to the reaction between the azetidinium groups of EMPA and the amino groups of SM (Gao et al., 2015; Zhong et al., 2007). The acetaldehyde value test in Fig. 4B shows that ambient-aged SMs had fewer crosslinkable amino groups. As a result, adhesive prepared with ambient-aged SM had a lower crosslinking density due to the insufficient amino groups and the uneven penetration of the crosslinker into SM, as confirmed by the even-increasing sol content of cured SM-based adhesive in Table 4. These facts indicated that the crosslinking density had much more impact on the bond strength and water resistance of SM adhesive than wettability.

TGA analysis showed that the cured adhesive had decreased mass residue (Fig. 5A) and a lower decomposition temperature in the main DTG peak (Fig. 5B) after ambient aging, which further evidenced the lowered crosslinking density of the SM-based adhesive prepared with ambient-aged SMs. In addition to the three traditional decomposition peaks of soybean-based adhesive at 20–120 °C (peak I assigned to water evaporation), 120–210 °C (peak II, referred to adhesive postcuring) and 210–360 °C (peak III, associated with adhesive decomposition) (Li et al.,

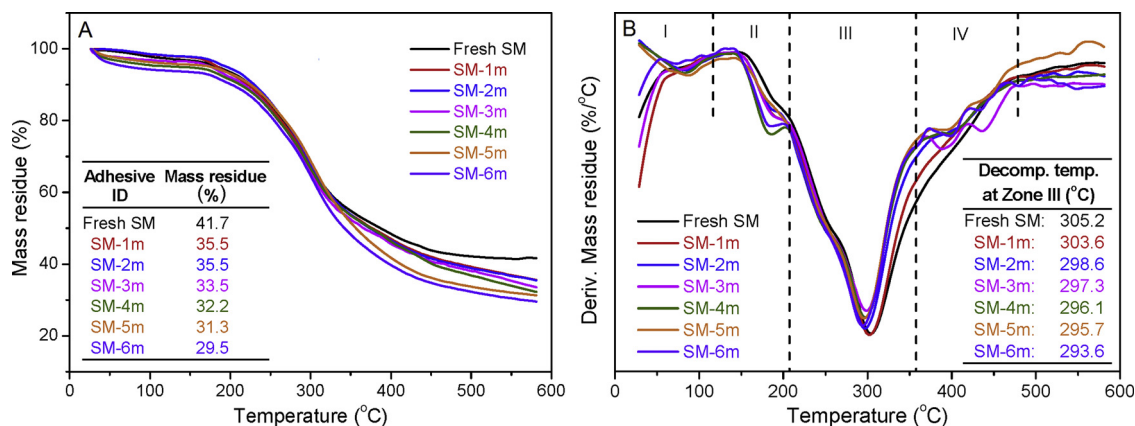


Fig. 5. TGA analysis of SM-based adhesives with various ambient-aged SMs.

2015a; Zhang et al., 2017), one new peak at 360–480 °C was observed in adhesives prepared with SM aged for more than 1 month, associated with the repolymerization of SM during ambient aging as confirmed by GPC analysis in Fig. 4A and XPS analysis in Table 2.

#### 4. Conclusions

The ambient aging of SM powder during storage was confirmed to lead to important changes of the structure and properties of SMs and SM-based adhesives. Due to the oxidization, decomposition, repolymerization and rearrangement of SM chains during ambient aging, SM had increased carbonyl content, amide content, average MW and crystallinity but decreased amino content upon the ambient-aging time. The SM-based adhesive prepared with ambient-aged SM showed decreasing bond strength, water resistance, contact angle, adhesive viscosity, bonded water content, thermal stability and crosslinking density. As the ambient aging time increased, the amino groups of SM decreased from 0.061 mmol/g to 0.048 mmol/g due to the repolymerizations between SM chains, causing decreased crosslinking density that led to deteriorated bond strength and water resistance of adhesive prepared with the ambient-aged SM. Due to the significant decrease of water resistance (soaked wet strength decreased from 1.46 MPa to 1.13 MPa in 5 months and aged wet strength decreased from 0.93 MPa to 0.72 MPa in 2 months), the storage time of SM should be less than 5 months for formulating SM-based adhesive for Type II plywood, while it should be less than 2 months for Type I plywood. The structure-property variations of SM and SM-based adhesive resulting from ambient aging should be considered in the case where SM for adhesives or other polymeric materials are stored longer than 2 months.

#### Declaration of Competing Interest

None.

#### Acknowledgments

This work was supported by the National Natural Science Foundation of China (grant number 31870542), the Fundamental Research Funds for the Central Universities (2572018CP01), the Research Program of Technological Innovation Alliance of Wood and Bamboo Industry (TIAWBI201904), and the Forest Intellectual Property Transformation Project (< GN4 > KJZZZZ2019006) < /GN4 > .

#### References

- Al-Qadiri, H., 2011. Fourier Transform Infrared (FT-IR) Spectroscopy. Lambert Academic Publishing, Saarbrücken.
- Bai, Y., Gao, Z., 2011. The ambient aging of wood fiber and its effect on mechanical properties of MDF panels. *Wood Sci. Technol.* 45, 501–510.
- Catalgol, B., Sozen, E., Bozaykut, P., Kaga, E., Kartal Ozer, N., Grune, T., 2012. The role of heat shock proteins in the protein oxidation during aging. *Free Radic. Bio. Med.* 5, S73–S74.
- Ciannamea, E., Stefani, P., Ruseckaite, R., 2015. Storage-induced changes in functional properties of glycerol plasticized-Soybean protein concentrate films produced by casting. *Food Hydrocoll.* 45, 247–255.
- Frihart, C.R., Satori, H., 2013. Soy flour dispersibility and performance as wood adhesive. *J. Adhes. Sci. Technol.* 27, 2043–2052.
- Fahmy, Y., El-Wakil, N., El-Gendy, A., Abou-Zeid, R., Youssef, M., 2010. Plant proteins as binders in cellulosic paper composites. *Int. J. Biol. Macromol.* 47, 82–85.
- Fan, B., Zhang, L., Gao, Z., Zhang, Y., Shi, J., Li, J., 2016. Formulation of a novel soybean protein-based wood adhesive with desired water resistance and technological applicability. *J. Appl. Polym. Sci.* 133, 43586.
- Gao, Q., Shi, S., Zhang, S., Li, J., Wang, X., Ding, W., Liang, K., Wang, J., 2012. Soybean meal-based adhesive enhanced by MUF resin. *J. Appl. Polym. Sci.* 125, 3676–3681.
- Gao, Z., Zhang, Y., Fang, B., Zhang, L., Shi, J., 2015. The effects of thermal-acid treatment and crosslinking on the water resistance of soybean protein. *Ind. Crop Prod.* 74, 122–131.
- Ghahri, S., Pizzi, A., 2018. Improving soy-based adhesives for wood particleboard by tannins addition. *Wood Sci. Technol.* 52, 261–279.
- Ghahri, S., Pizzi, A., Mohebbi, B., Mirshoktaie, A., Mansouri, H.R., 2018a. Soy-based, tannin-modified plywood adhesives. *J. Adhes.* 94, 218–237.
- Ghahri, S., Pizzi, A., Mohebbi, B., Mirshoktaie, A., Mansouri, H.R., 2018b. Improving water resistance of soy-based adhesive by vegetable tannin. *J. Polym. Environm.* 26, 1881–1890.
- Gu, K., Li, K., 2011. Preparation and evaluation of particleboard with a soy flour-poly-ethylenimine-maleic anhydride adhesive. *J. Am. Oil Chem. Soc.* 88, 673–679.
- Guerrero, P., Etxabide, A., Leceta, I., Peñalba, M., Caba, K., 2014. Extraction of agar from *Gelidium sesquipedale* (Rhodophyta) and surface characterization of agar based films. *Carbohydr. Polym.* 99, 491–498.
- Guerrero, P., Garrido, T., Leceta, I., Caba, K.D.L., 2013. Films based on proteins and polysaccharides: preparation and physical-chemical characterization. *Eur. Polym. J.* 49, 3713–3721.
- Haque, E., Bhandari, B., Gidley, M., Deeth, H., Whittaker, A., 2015. Change in molecular structure and dynamics of protein in milk protein concentrate powder upon ageing by solid-state carbon NMR. *Food Hydrocoll.* 44, 66–70.
- Hipkiss, A., Brownson, C., Carrier, M., 2001. Carnosine, the anti-ageing, anti-oxidant dipeptide, may react with protein carbonyl groups. *Mech. Ageing Dev.* 122, 1431–1445.
- Huang, W., Sun, X., 2000. Adhesive properties of soy proteins modified by sodium dodecyl sulfate and sodium dodecylbenzene sulfonate. *J. Am. Oil Chem. Soc.* 77, 705–708.
- Kumar, R., Choudhary, V., Mishra, S., Varma, I., Mattiason, B., 2002. Adhesives and plastics based on soy protein products. *Ind. Crop Prod.* 16, 155–172.
- Lei, H., Du, G., Wu, Z., Xi, X., Dong, Z., 2014. Cross-linked soy-based wood adhesives for plywood. *Int. J. Adhes. Adhes.* 50, 199–203.
- Li, J., Li, X., Li, J., Gao, Q., 2015a. Investigating the use of peanut meal: a potential new resource for wood adhesives. *RSC Adv.* 5, 80136–80141.
- Li, J., Zhang, B., Li, X., Yi, Y., Shi, F., Guo, J., Gao, Z., 2019. Effects of typical soybean meal type on the properties of soybean-based adhesive. *Int. J. Adhes. Adhes.* <https://doi.org/10.1016/j.ijadhadh.2019.01.010>.
- Li, N., Prodyawonga, S., He, Z., Sun, X., Wang, D., 2017. Effect of drying methods on the physicochemical properties and adhesion performance of water-washed cottonseed meal. *Ind. Crops Prod.* 109, 281287.
- Li, Y., Chen, F., Zhang, L., Yao, Y., 2015b. Effect of surface changes of soy protein materials on water resistance. *Mater. Lett.* 149, 120–122.
- Liu, H., Li, C., Sun, X.S., 2017. Soy-oil-based waterborne polyurethane improved wet strength of soy protein adhesives on wood. *Int. J. Adhes. Adhes.* 73, 66–74.
- Liu, M., Wang, Y., Wu, Y., He, Z., Wan, H., 2018. “Greener” adhesives composed of urea-formaldehyde resin and cottonseed meal for wood-based composites. *J. Cleaner Prod.* 187, 361–371.
- Liu, Y., Li, K., 2007. Development and characterization of adhesives from soy protein for bonding wood. *Int. J. Adhes. Adhes.* 27, 59–67.
- Luo, J., Li, X., Zhang, H., Gao, Q., Li, J., 2017. Properties of a soybean meal-based plywood adhesive modified by a commercial epoxy resin. *Int. J. Adhes. Adhes.* 71, 99–104.
- Mo, X., Sun, X., 2003. Effects of storage time on properties of soybean protein-based plastics. *J. Polym. Environ.* 11, 15–22.
- Park, B., Lee, S., Roh, J., 2009. Effects of formaldehyde/urea mole ratio and melamine content on the hydrolytic stability of cured urea-melamine-formaldehyde resin. *Eur. J. Wood Prod.* 67, 121–123.
- Qin, Z., Gao, Q., Zhang, S., Li, J., 2013. Glycidyl methacrylate grafted onto enzyme-treated soybean meal adhesive with improved wet shear strength. *Bioresources* 8, 5369–5379.
- Reeg, S., Grune, T., 2015. Protein oxidation in aging: does it play a role in aging progression? *Antioxid. Redox. Sign.* 23, 239–255.
- Sitz, E.D., Bajwa, D.S., Webster, D.C., Monono, E.M., Wiesenborn, D.P., Bajwa, S.G., 2017. Epoxidized sucrose soyate—a novel green resin for crop straw based low density fiberboards. *Ind. Crops Prod.* 107, 400–408.
- Tabarsa, T., Jahanshahi, S., Ashori, A., 2011. Mechanical and physical properties of wheat straw boards bonded with a tannin modified phenol-formaldehyde adhesive. *Compos. Part B* 42, 176–180.
- Tous, L., Ruseckaite, R.A., Ciannamea, E.M., 2019. Sustainable hot-melt adhesives based on soybean protein isolate and polycaprolactone. *Ind. Crops Prod.* 135, 153–158.
- Vnucce, D., Kutnar, A., Gorsek, A., 2017. Soy-based adhesives for wood-bonding—a review. *J. Adhes. Sci. Technol.* 31, 910–931.
- Wang, G., Chen, H., 2014. Carbohydrate elimination of alkaline-extracted lignin liquor by steam explosion and its methylolation for substitution of phenolic adhesive. *Ind. Crop Prod.* 53, 93–101.
- Zhang, P., Li, Y., Li, F., Qu, Y., Lin, Q., Chen, N., 2017. Development of defatted soy flour-based adhesives by acid hydrolysis of carbohydrates. *Polymers* 9, 153.
- Zhao, S., Wang, Z., Kang, H., Li, J., Zhang, S., Han, C., Huang, A., 2018. Fully bio-based soybean adhesive in situ cross-linked by interactive network skeleton from plant oil-anchored fiber. *Ind. Crops Prod.* 122, 366–374.
- Zhao, X., Zhu, H., Zhang, B., Chen, J., Ao, Q., Wang, X., 2015. XRD, SEM, and XPS analysis of soybean protein powders obtained through extraction involving reverse micelles. *J. Am. Oil Chem. Soc.* 92, 975–983.
- Zhong, Z., Sun, X., 2000. Thermal behavior and nonfreezing water of soybean protein components. *Cereal Chem.* 77, 495–500.
- Zhong, Z., Sun, X., Wang, D., 2007. Isoelectric pH of polyamide-epichlorohydrin modified soy protein improved water resistance and adhesion properties. *J. Appl. Polym. Sci.* 103, 2261–2270.